Please cite this article in press as: Adams et al., Drug Tolerance in Replicating Mycobacteria Mediated by a Macrophage-Induced Efflux Mechanism, Cell (2011), doi:10.1016/j.cell.2011.02.022

Cell

Drug Tolerance in Replicating Mycobacteria Mediated by a Macrophage-Induced Efflux Mechanism

Kristin N. Adams,[1,5] Kevin Takaki,[1,5] Lynn E. Connolly,[2,6,7] Heather Wiedenhoft,[1,6] Kathryn Winglee,[1,6,8] Olivier Humbert,[1] Paul H. Edelstein,[4] Christine L. Cosma,[1] and Lalita Ramakrishnan[1,2,3,*]
[1]Department of Microbiology
[2]Department of Medicine
[3]Department of Immunology
University of Washington, Seattle, WA 98195, USA
[4]Department of Pathology and Laboratory Medicine, University of Pennsylvania School of Medicine, Philadelphia, PA 19104, USA
[5]These authors contributed equally to this work
[6]These authors contributed equally to this work
[7]Present address: Department of Medicine, Division of Infectious Diseases and Microbiology and Immunology, Program in Microbial Pathogenesis and Host Defense, University of California, San Francisco, San Francisco, CA 94143, USA
[8]Present address: Center for Tuberculosis Research, Department of Medicine, Johns Hopkins University, Baltimore, MD 21218, USA
*Correspondence: lalitar@uw.edu
DOI 10.1016/j.cell.2011.02.022

SUMMARY

Treatment of tuberculosis, a complex granulomatous disease, requires long-term multidrug therapy to overcome tolerance, an epigenetic drug resistance that is widely attributed to nonreplicating bacterial subpopulations. Here, we deploy *Mycobacterium marinum*-infected zebrafish larvae for in vivo characterization of antitubercular drug activity and tolerance. We describe the existence of multidrug-tolerant organisms that arise within days of infection, are enriched in the replicating intracellular population, and are amplified and disseminated by the tuberculous granuloma. Bacterial efflux pumps that are required for intracellular growth mediate this macrophage-induced tolerance. This tolerant population also develops when *Mycobacterium tuberculosis* infects cultured macrophages, suggesting that it contributes to the burden of drug tolerance in human tuberculosis. Efflux pump inhibitors like verapamil reduce this tolerance. Thus, the addition of this currently approved drug or more specific efflux pump inhibitors to standard antitubercular therapy should shorten the duration of curative treatment.

INTRODUCTION

Despite more than 50 years of effective antitubercular drugs, tuberculosis (TB) eradication remains elusive (Sacchettini et al., 2008) due to the complexity of curative treatment regimens (Connolly et al., 2007; Donald and McIlleron, 2009). Long-term therapy is required to prevent relapses with genetically drug-sensitive bacilli that become transiently resistant in the host, a phenomenon called tolerance. The best-case regimen of six months was made possible by drug combinations that presumably reduce the tolerant population (Donald and McIlleron, 2009). This so-called "short course therapy" represented a major advance, as prior regimens lasted 12–18 months. However, adherence to 6 months of multidrug treatment is difficult, leading to relapses that perpetuate the epidemic and fuel the development of genetic resistance (Sacchettini et al., 2008). Thus, an urgent goal of antitubercular drug discovery is to overcome tolerance (Connolly et al., 2007; Sacchettini et al., 2008). Several new drugs are in development (Sacchettini et al., 2008), yet most lack this key treatment-shortening property. This failure highlights a poor understanding of TB tolerance mechanisms (Barry et al., 2009; Connolly et al., 2007; Sacchettini et al., 2008; Warner and Mizrahi, 2006).

Drug tolerance in TB is best contextualized to the in vivo lifestyle of mycobacteria. *Mycobacterium tuberculosis* (Mtb) resides within complex immunological structures called granulomas, either within macrophages or extracellularly, in the necrotic core (caseum) (Figure S1 available online) (Barry et al., 2009; Connolly et al., 2007). Multiple granuloma types, reflecting different levels of local disease activity, may coexist in a given patient (Figure S1) (Barry et al., 2009; Canetti, 1955; Connolly et al., 2007; Rich, 1946). A longstanding model is that tolerant bacteria are sequestered in a subset of granulomas wherein their replication and metabolism are uniformly slowed (Figure S1) (Barry et al., 2009; Connolly et al., 2007). Newer models posit that quiescent, drug-tolerant bacteria are present in all lesion types and may be induced by deterministic mechanisms that are responsive to stress (e.g., hypoxia) and/or the stochastic formation of persister cells, some of which may be nonculturable under standard laboratory conditions (Figure S1) (Barry et al., 2009; Connolly et al., 2007; Garton et al., 2008; Mukamolova

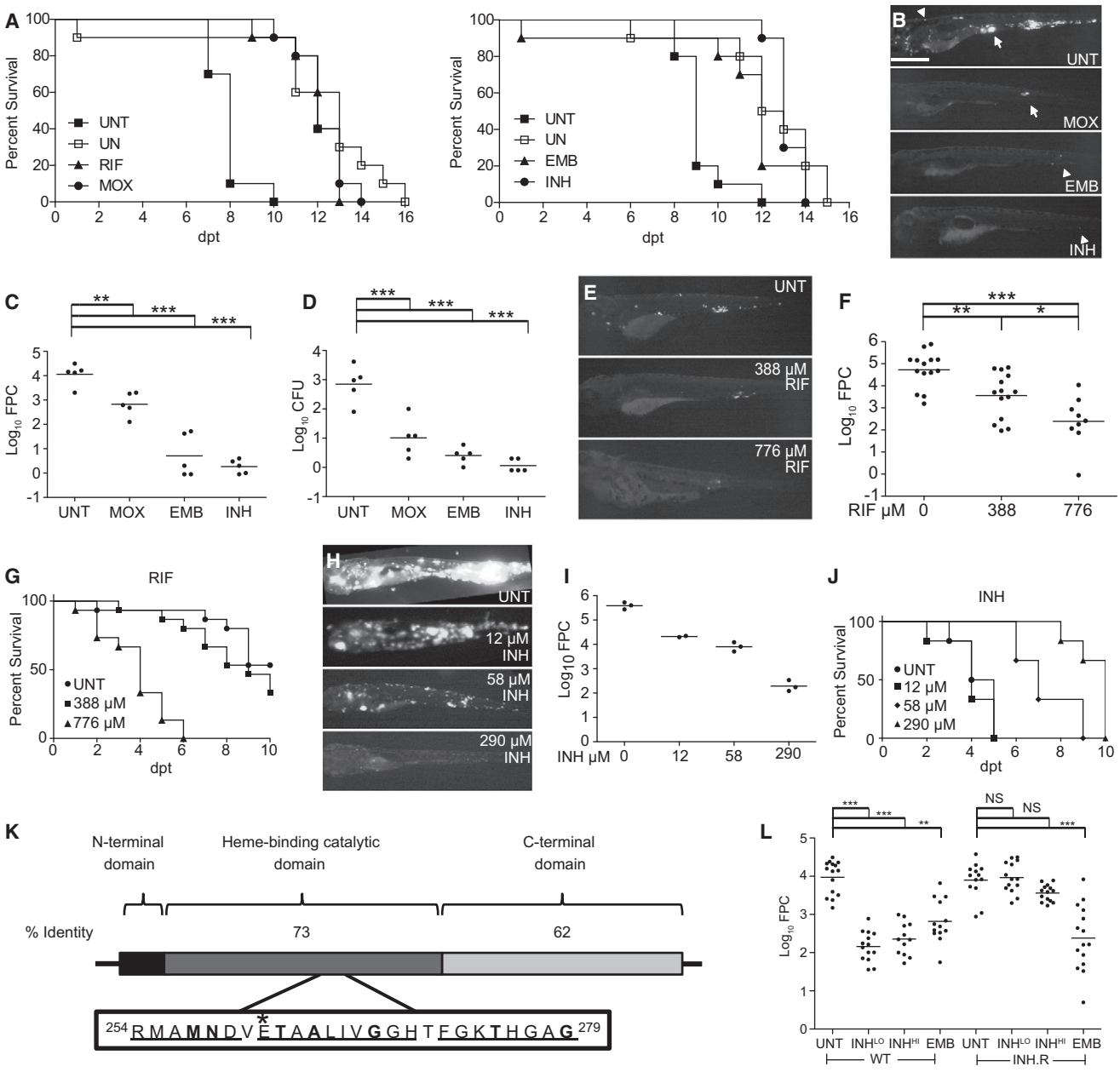

Figure 1. The Mm-Larval Zebrafish Infection Model Replicates the Specificity and Activity of Clinically Relevant Antitubercular Drugs

(A–D) Larvae were soaked in the MEC of RIF (388 μM), MOX (62.3 μM), EMB (1442 μM), or INH (290 μM) (Table S1).

(A) Survival of uninfected (UN) larvae versus those infected with 800 Mm and immediately treated with RIF, MOX, EMB, INH, or left untreated (UNT). (Left) In the presence of 1% DMSO (see Figure S2A). Survival of treated infected larvae was significantly different from UNT larvae for all drugs (Table S2). Results are representative of at least two independent experiments.

(B–D) Larvae were infected with 155 Mm and left untreated (UNT) or treated with MOX, EMB, or INH for 4 days prior to assessment of bacterial burdens by fluorescence microscopy (B, representative larvae are shown), FPC (C), or CFU enumeration of the lysed larvae immediately after imaging (D). Arrow, granuloma; arrowhead, single infected macrophage. Scale bar, 500 μm. For (C) and (D), individual larvae (points) and means (bars) are shown. Significance testing by one way ANOVA with Dunnett's post test.

(E and F) Larvae infected with 46 Mm were soaked for 3 days in 388 or 776 μM RIF or were left untreated. Representative fluorescence images (E) and bacterial burdens (F) of survivors are shown. Significance testing by one-way ANOVA with Tukey's posttest.

(G) Survival of uninfected larvae upon treatment with 0, 388, or 776 μM RIF added 2 days postfertilization (dpf). p = 0.0010 for 0 versus 776; 0 versus 388 μM was not significant (NS) by Log-rank test. n = 15 per group.

(H–J) Larvae infected with 1800 Mm were left untreated or immediately soaked in 12, 58, or 290 μM INH. Representative fluorescence images (H) and bacterial burdens (I) of survivors at 4 dpt are shown. Mean bacterial burdens (bars) compared by one-way ANOVA with Tukey's posttest resulted in p < 0.001 for all

et al., 2010; Sacchettini et al., 2008; Warner and Mizrahi, 2006). However, all tolerance models and consequently drug discovery efforts are centered on the assumption that slowed growth and/or metabolic quiescence is the primary mediator of tolerance.

In this study, we demonstrate that growing mycobacteria develop multidrug tolerance soon after they infect macrophages. This understanding was gained by a two-pronged approach. First, we used zebrafish larvae infected with *Mycobacterium marinum* (Mm) to spatially and temporally characterize the responses of individual animals to frontline antitubercular drugs. Mm infections feature drug tolerance and require long-term treatment in both humans and fish (Aubry et al., 2002; Decostere et al., 2004). Using the larval model, we discovered that tolerant bacteria arise within individual macrophages soon after infection and are then expanded and disseminated by tuberculous granulomas. Guided by these findings, we used cultured macrophage infection models combined with bacterial efflux pump mutants and pharmacological inhibitors to identify both a mechanism and a therapy for macrophage-induced tolerance in TB.

RESULTS

A Zebrafish Larval Model for In Vivo Characterization of Antitubercular Drug Activity

To assess antitubercular drug activity in the model, we infected larvae intravenously with GFP-expressing Mm and maintained them in the presence of antitubercular drugs. Concentrations that represented multiples of the in vitro minimum inhibitory concentration (MIC) for Mm were used, and the drug-supplemented water was changed daily (Table S1, Figures S2A–S2E, and Experimental Procedures). We established minimal isoniazid (INH), rifampicin (RIF), ethambutol (EMB), and moxifloxacin (MOX) concentrations that were nontoxic and normalized host survival when administered within 1 day postinfection (dpi), which we term the minimum effective concentration (MEC) (Figure 1A, Figures S2B–S2E, Table S1, and Table S2). Bacterial burdens of infected larvae can be assessed visually by fluorescence microscopy or quantitatively by larval lysis and enumeration of bacterial colony-forming units (CFU). To facilitate rapid, serial quantification of bacterial burden, we developed software that enumerates fluorescent pixels in images of infected larvae, or fluorescent pixel count (FPC), and showed it to be an accurate predictor of bacterial burden (Figure S3 and Experimental Procedures). Increased survival was associated with lower bacterial burdens at 4 days posttreatment (dpt), as judged by fluorescence microscopy, and was confirmed quantitatively by FPC and CFU analyses (Figures 1A–1F, Figure S3, and Table S2). Findings that were consistent with human TB data were also obtained with streptomycin (STM, Figures S2C–S2E), which has resurged as a cornerstone of treatment for extremely drug-resistant (XDR) TB (Donald and McIlleron, 2009). In summary, clinically relevant antitubercular drugs were efficacious in the zebrafish infection model, with the expected exception of pyrazinamide, to which Mm is innately resistant (Figures S2F and S2G).

To further probe the model's relevance to human TB, we used the MECs as starting points from which to examine drug potency and dose-dependent activity. In human pulmonary TB studies, the early bactericidal activity (EBA) of antitubercular drugs, defined as their ability to reduce sputum bacterial counts in pulmonary TB patients over the first several days, has been useful to guide drug dosing (Donald and Diacon, 2008; Jindani et al., 2003). Each drug has distinctive EBA characteristics. For RIF, doses greater than the currently used therapeutic dose increase the EBA, raising the question of whether higher doses would have greater efficacy (Donald and Diacon, 2008). In the larvae, treatment with the RIF MEC caused a 1.2 $\log_{10}$ reduction in bacterial burden, whereas treatment with twice the MEC caused an additional 1.2 $\log_{10}$ reduction despite increased toxicity (Figures 1E–1G). We similarly observed dose-dependent activity for MOX: stepwise increases in concentration produced greater diminutions in bacterial burdens (Figure S2H). In contrast to RIF, INH EBA does not increase when the conventional dose is doubled. We also observed no further reduction in bacterial counts at double the INH MEC (data not shown). Further, stepwise 2-fold reductions from the conventional dose continue to show activity in human TB, with a graded EBA decrease down to 1/16th the therapeutic dose (Donald and Diacon, 2008). Similarly, we found a graded concentration-dependent bactericidal activity down to 1/24th the MEC (Figures 1H and 1I) and a therapeutic benefit at 1/5th the MEC (Figure 1J).

Finally, because drug-resistant TB is an increasing problem (Sacchettini et al., 2008), we asked whether the model could differentiate Mm strains with altered drug susceptibility. INH resistance is usually the first to occur in human TB and often the first step in the progression to XDR TB (Donald and McIlleron, 2009). INH is a prodrug activated by the bacterial catalase KatG, and the vast majority of INH-resistant clinical Mtb isolates have *katG* mutations (Sandgren et al., 2009). We identified a spontaneous INH-resistant Mm *katG* mutant with an in vitro INH MIC of 464 μM, 8-fold higher than for wild-type (Figure 1K and Extended Experimental Procedures). The relative resistance of the Mm *katG* mutant was detectable in vivo: in larvae infected with wild-type Mm, maximal bacterial killing was observed at 290 μM, whereas an 8-fold higher concentration was ineffective against the *katG* mutant (Figure 1L). INH resistance was specific: EMB, which has a distinct target (Belanger et al., 1996), showed similar efficacy against both strains (Figure 1L). In summary, the zebrafish larval model reliably replicates the activity of antitubercular compounds and their dosing characteristics in humans.

comparisons, with the exception of 12 versus 58 μM INH, which was not significant ($p > 0.05$). (J) Survival curve, n = 6 larvae per group. $p = 0.0018$, log-rank test for trend comparing all curves; $p = 0.0010$ for comparison of UNT versus 58 μM or UNT versus 290 μM.

(K) Functional domains of KatG. Mtb KatG is 740 aa, and Mm KatG is 743 aa. Boxed inset of Mtb catalytic domain shows regions of identity with Mm (underlined) and point mutations (in bold) that confer INH resistance in Mtb (Sandgren et al., 2009). *Position of the single amino acid substitution (E265V) in the INH-resistant Mm strain corresponds to the E261 position of Mtb KatG.

(L) Bacterial burdens of 3 dpt larvae infected with 300 WT or INH-resistant (INH.R) Mm and soaked in 290 (LO) or 2320 μM (HI) INH, 1442 μM EMB, or left UNT beginning 1 dpi. Median $\log_{10}$FPC (bars) compared using Kruskal-Wallis test with Dunn's posttest.

*$p < 0.05$; **$p < 0.01$; ***$p < 0.001$. NS, not significant.

Drug Tolerance Occurs Prior to Granuloma Formation

Our observation that residual cultivatable bacteria persisted 4 dpt, despite initiating treatment within a day of infection when the bacteria were in individual macrophages (Figures 1B–1D), suggested the early presence of drug-tolerant bacteria, prior to granuloma formation. We pursued this observation in detail for INH because its tolerance in human TB has been studied extensively (Donald and Diacon, 2008; Donald and McIlleron, 2009; Jindani et al., 2003). We confirmed that the residual bacteria were tolerant, rather than genetically resistant, to INH: the INH susceptibility of individual bacilli recovered from six treated larvae (10.3 ± 1.2 CFU per larva) was unchanged from the parental strain.

INH tolerance is seen in human EBA studies in which monotherapy produces biphasic killing. The majority of the bacteria are killed with 2 days of treatment, after which the rate of killing drops, leaving a population of drug-tolerant bacteria 14 dpt (Figure 2A) (Donald and Diacon, 2008; Jindani et al., 2003). We conducted an EBA-like study in the larvae, starting treatment after granulomas had formed, at 3 dpi. Serial quantitative tracking of infection by fluorescence microscopy revealed that INH killing kinetics mirror those observed in human EBA studies (Figures 2A–2C).

By tracking individual animals, we determined the location of the persistent bacteria (Figure 2B). Several infected macrophages had very little diminution in fluorescence, suggesting that they contained tolerant bacteria, and their varying positions on consecutive days suggested their continued movement during treatment. There were also residual infected macrophages (Figure 2B, arrowhead) from granulomas that had dissolved with treatment (Figure 2B, arrow). Thus, tolerant bacteria were present both in individual macrophages and in granuloma macrophages.

In human TB, the addition of RIF to INH-containing regimens has shortened time to sterilization and thus treatment length. This is reflected in EBA studies in which RIF is not rapidly bactericidal on its own and the additional activity of the INH-RIF combination is seen only in the slower phase of killing, when INH-tolerant bacteria are implicated (Figure 2A) (Donald and Diacon, 2008; Jindani et al., 2003). Therefore, RIF's treatment-shortening effect is attributed to its capacity to reduce INH-tolerant bacteria (Donald and McIlleron, 2009). Reminiscent of the human data, RIF in the larvae was not rapidly bactericidal on its own (Figure 2D), yet it increased INH efficacy in the slow phase of its EBA curve (Figure 2E). Residual bacteria persisted after combination therapy, albeit fewer than with INH monotherapy (Figure 2F). In sum, the model demonstrates drug tolerance akin to that seen in human TB and the well-known synergistic effect of RIF in reducing tolerance. Furthermore, it reveals tolerant bacteria within individual macrophages at the earliest stages of infection.

Drug-Tolerant Bacteria Are Expanded and Disseminated by Granuloma Formation

All models of TB tolerance invoke metabolically quiescent bacteria (Barry et al., 2009; Connolly et al., 2007; Sacchettini et al., 2008; Warner and Mizrahi, 2006). Yet during human TB treatment, individual lesions can expand, or new ones appear at distant sites, despite overall clinical improvement and reduction in lesion size and number (Akira et al., 2000; Barry et al., 2009; Bobrowitz, 1980; Canetti, 1955). Importantly, bacteria from new lesions are drug sensitive, and the patients are ultimately cured with no change in therapy (reviewed in Akira et al., 2000). These observations are consistent with an uneven distribution of drug-tolerant bacteria that expand locally or after dissemination. Indeed, even before the advent of effective TB therapy, it was appreciated that, within a given patient, some lesions resolve while others worsen, suggesting distinct local host responses in the course of natural infection (Canetti, 1955; Rich, 1946).

We wondered whether the drug-tolerant bacteria that we had observed within scattered macrophages are the ones that are then amplified and disseminated by mechanisms of granuloma formation (Davis and Ramakrishnan, 2009). However, we first had to determine whether our model recapitulated the differential progression of natural infection. We found that, in the first week of infection, some granulomas progressed while others resolved (Figure 3A). Lesions in the head region (containing the organs) were more likely to progress, whereas those in the tail region (primarily muscle) were more likely to resolve (Figures 3B and 3C). The effect was even more striking at later developmental stages (days 7 to 11), when organogenesis is more advanced (Figure 3C). By 1 month, granulomas were exclusively within organs (Figure 3D and 3E), reminiscent of the observation that human TB seldom involves muscle (Rich, 1946).

Next, to study the effect of drug treatment on individual lesions, we infected larvae with a range of inocula to achieve varying infection burdens (Figure 3F) and then began INH treatment for half of the larvae. We quantified and spatially localized infection in each animal at the start of treatment and 3 days later by fluorescence microscopy. As expected, untreated larvae demonstrated an increase in bacterial burden (+0.2176 $\log_{10}$ FPC, $p = 0.0008$, Student's t test), whereas treatment reduced the bacterial burden (-1.001 $\log_{10}$ FPC).

Spatial monitoring of the untreated larvae confirmed the expected differential progression of lesions. Ten of the 12 treated larvae had a reduction in bacterial burdens ranging from 32.3% to 99.7% (Figures 3F and 3G). We found local "nonresponsiveness" among the responding larvae, analogous to that observed in humans (Figures 3G–3I). For example, fish 11 (Figures 3G and 3H) had an overall 32.3% reduction in bacterial burden, yet two individual infected macrophages expanded into two infected cells and a granuloma and multiple new foci appeared. New foci developed even in animals with an overall >90% reduction in bacterial burdens (e.g., fish 5, Figures 3G and 3I).

Finally, we determined whether new infection foci resulted from the egress of macrophages (containing tolerant bacteria) from existing granulomas, a phenomenon that we have documented during untreated infection (Davis and Ramakrishnan, 2009). We infected larvae with bacteria expressing the fluorescent reporter Kaede that changes from green to red upon photoactivation (Davis and Ramakrishnan, 2009). We selectively photoactivated the largest granuloma and immediately began INH treatment (Figure 3J, left). We then assessed whether macrophages harboring the photoactivated bacteria left granulomas

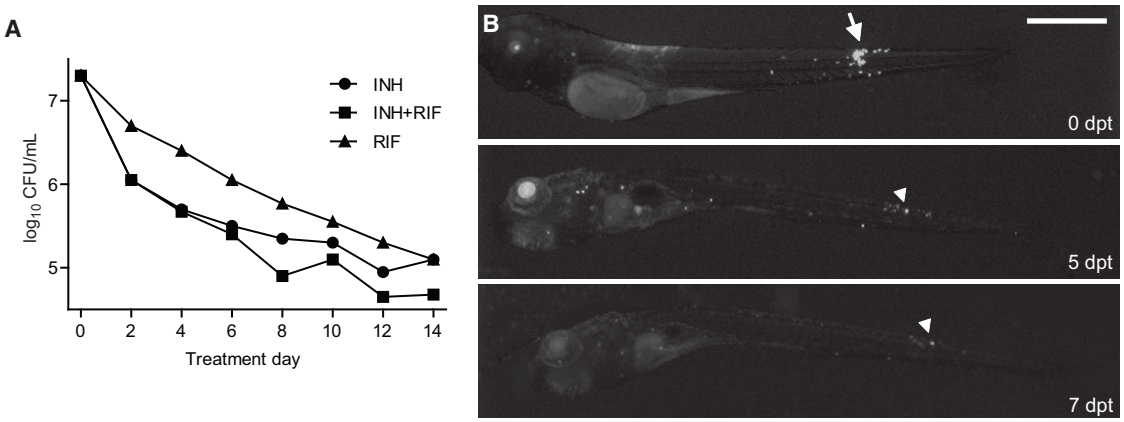

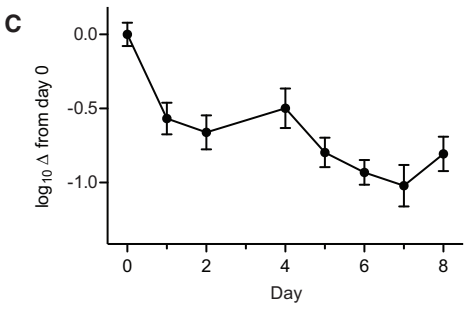

	Δ/d	sd	N
EBA_{0-2}	0.33	0.24	19
EBA_{2-7}	0.06	0.14	11
EBA_{0-7}	0.14	0.07	11

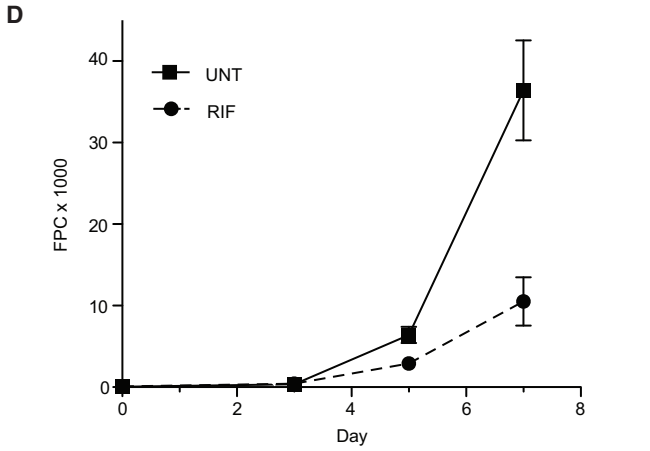

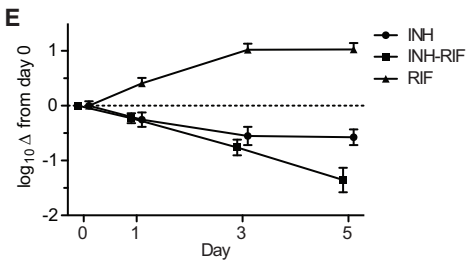

	INH			INH-RIF		
	Δ/d	sd	N	Δ/d	sd	N
EBA_{0-5}	0.12	0.079	10	0.27	0.14	8
EBA_{1-5}	0.08	0.095	10	0.28	0.14	8

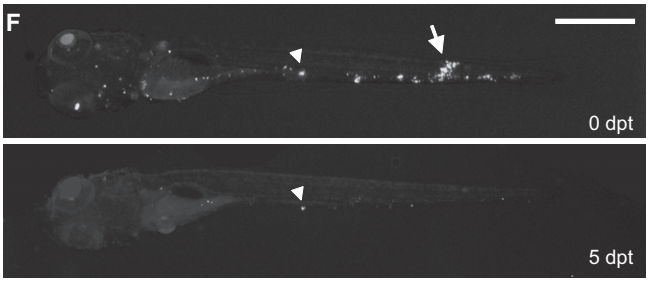

Figure 2. INH Treatment of Mm-Infected Larvae Results in a Biphasic EBA with Persistence of Tolerant Organisms

(A) Authors' rendition of human clinical EBA data (see Figure 1 of Jindani et al., 2003) showing the rate of clearance of Mtb from sputum in patients with previously untreated, smear-positive pulmonary tuberculosis upon treatment with INH and/or RIF.

(B and C) Twenty larvae were infected with 300 Mm and treated with 290 μM INH beginning 3 dpi. Each larva was imaged daily for 8 dpt, and bacterial burdens were quantified by FPC.

(B) Representative larva imaged at the beginning of treatment (0 dpt) and again at 5 and 7 dpt. Arrow, granuloma; arrowhead, a macrophage that contains persistent bacteria.

(C) EBA curve for INH-treated larvae showing the mean $\log_{10}$ FPC change from day 0, calculated as described in the Experimental Procedures. Error bars represent SEM. Δ/d is the decrease in bacterial burden per day, expressed as $\log_{10}$, over the specified time period.

(D–F) Ten larvae per group were infected with 300 Mm and were serially imaged for enumeration of bacterial burden by FPC.

(D) Larvae were treated with 388 μM RIF or left untreated, beginning 1 dpi. Mean FPC and SEM are shown.

(E) Larvae were treated with 290 μM INH, 388 μM RIF, or a combination of both drugs beginning at 3 dpi. Data analyzed as in (C). Error bars represent SEM. Δ/d is the decrease in bacterial burden per day, expressed as $\log_{10}$, over the specified time period.

(F) Representative INH-RIF treated larvae annotated as in (B).

Please cite this article in press as: Adams et al., Drug Tolerance in Replicating Mycobacteria Mediated by a Macrophage-Induced Efflux Mechanism, Cell (2011), doi:10.1016/j.cell.2011.02.022

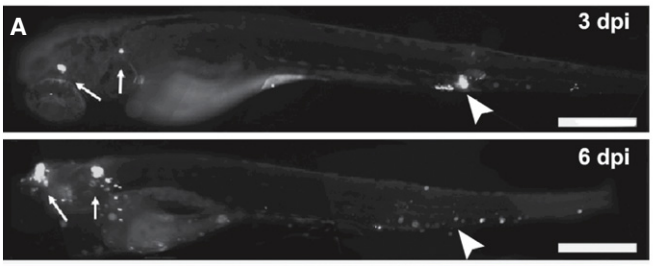

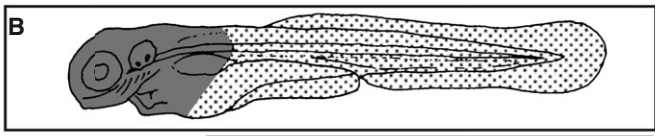

C

Granuloma site	Days 4-7		Days 7-11	
	Enlarged	Reduced	Enlarged	Reduced
Head	6	3	10	2
Tail	8	13	4	14

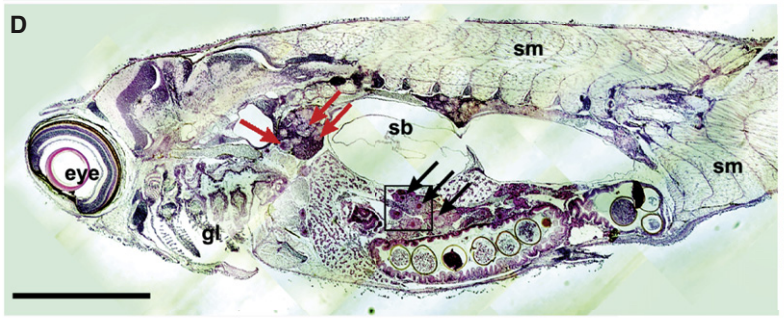

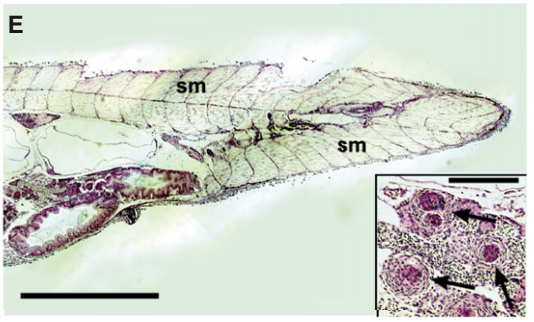

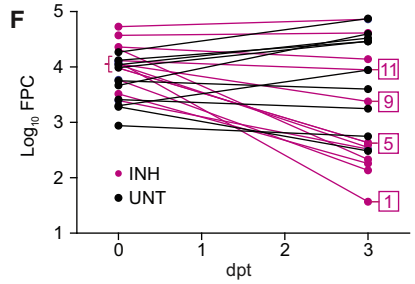

G

Fish	Panel	Pre-treatment burden (FPC)	Post-treatment burden (FPC)	Percent reduction	Number of expanded foci	Number of new foci
1		12260	37	99.7	0	4
5	I	9612	431	95.6	0	2
9		11346	2387	79.0	1	1
11	H	13065	8848	32.3	2	5

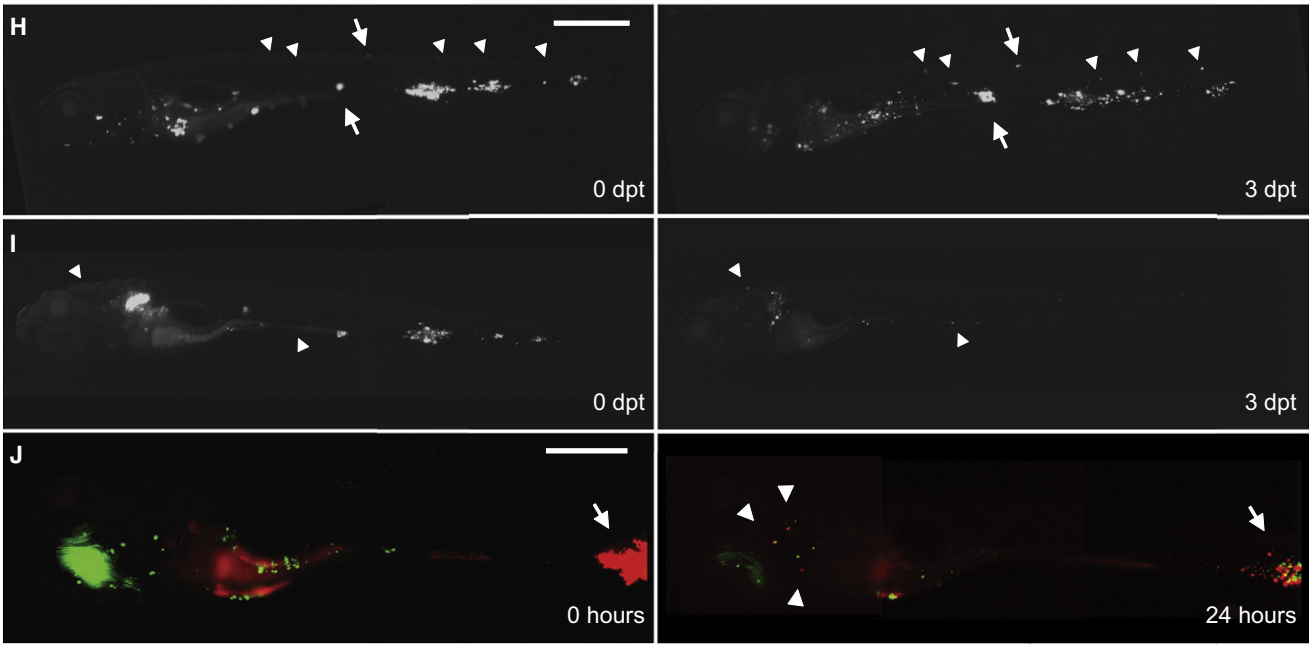

Figure 3. Mm Infections Are Dynamic during Antibiotic Treatment

(A–D) Tracking of untreated Mm infections in individual larvae.

(A) Fluorescence images of a representative larva at 3 and 6 dpi. Arrows, enlarging granulomas; arrowheads, shrinking granulomas. Scale bar, 400 μm.

(B) Cartoon indicating "head" region (gray) primarily containing organs and "tail" region (stippled) comprised mostly of muscle.

after initiating treatment. Within 24 hr, three infected macrophages had left the granuloma and dispersed far from the initial site (Figure 3J, right). Importantly, the original granuloma had shrunk substantially, showing its overall response to therapy, consistent with the human data (Bobrowitz, 1980). The bacteria within the departed macrophages were both red and green fluorescent, suggesting that they were synthesizing new Kaede protein and thus metabolically active, again consistent with the human data in which the new foci had viable bacteria that were then able to expand.

In summary, as is the case in human TB, individual lesions in Mm-infected zebrafish larvae respond variably to treatment, and dissemination occurs during effective therapy. The detailed temporal monitoring possible in this model suggests a mechanism for these longstanding observations in humans: drug treatment selects for tolerant bacteria residing within individual macrophages, which can expand into granulomas by recruiting new macrophages and/or migrate to disseminate infection.

Macrophage Residence Induces Drug Tolerance in Mm and Mtb

The drug-tolerant bacteria observed within larval macrophages can be explained by three nonmutually exclusive mechanisms: (1) pre-existing drug-tolerant persisters, (2) induction of tolerance upon exposure to the macrophage environment, and (3) induction of tolerance upon exposure to drug. Subtherapeutic concentrations of multiple drugs produce tolerance in actively growing Mtb cultures (de Steenwinkel et al., 2010; Morris et al., 2005; Viveiros et al., 2002), and we found this to also be the case for Mm (Figure S4A). To probe the mechanism(s) of tolerance in the context of host infection, we examined the development of INH tolerance in larvae depleted of macrophages by antisense knockdown of the PU.1 myeloid transcription factor; in the absence of macrophages, the Mm grow extracellularly (Clay et al., 2007). Wild-type and macrophage-depleted (PU.1) larvae were infected at 1 day postfertilization (dpf), and INH treatment was begun the following day. By 2 dpt, when INH tolerance is first apparent (Figure 2C), wild-type larvae had 10.4% ± 2.9% of the bacteria in the untreated controls, whereas PU.1-depleted larvae had 3.4% ± 0.7%, a 3.1-fold reduction (Figure 4A). The improved relative efficacy of INH in the PU.1-deficient larvae was even greater at 4 dpt, with a 5.7-fold relative reduction (1.9% ± 0.4% residual bacteria in wild-type versus 0.3% ± 0.07%) (Figure 4A). These data suggested that the tolerant bacterial population was enriched by macrophage residence.

To determine the mechanism of this macrophage-dependent tolerance, we turned to a cell culture infection model using J774A.1 mouse or THP-1 human macrophage cell lines (Volkman et al., 2004). Cells infected with Mm for either 2 or 96 hr were treated with 174 μM INH (3-fold the in vitro MIC) for an additional 48 hr and then lysed to obtain intracellular bacterial counts. After 2 hr of macrophage infection, 7.6% ± 0.8% Mm survived the subsequent 48 hr of INH treatment, whereas after a 96 hr infection period, 49.5% ± 8.1% survived treatment, representing a 6.5-fold increase in persisting bacteria (Figures 4B and 4C). There was no additional killing with 10-fold increased INH (1740 μM) (Figure 4C). The INH MIC for the bacteria recovered at 96 hr was unchanged from the parental strain, confirming that they had not acquired genetic resistance.

Our findings suggested that intramacrophage residence induces drug tolerance. Alternatively, drug activity could be limited intracellularly due to the residence of a bacterial subpopulation in a protected niche or to drug modification by the host cell. To differentiate between these possibilities, bacteria were grown in macrophages for 2 or 96 hr, released from the infected macrophages, and then incubated in bacterial growth medium with and without drugs for an additional 48 hr prior to plating. Even with direct exposure to 174 μM INH, the proportion of tolerant bacteria was > 200-fold higher at 96 hr postinfection (hpi) than after 2 hpi (Figure 4D and Table S3). Macrophage-conditioned Mm also developed tolerance to RIF with a 20.6-fold increase in survival and to MOX with a 4.8-fold increase in survival (Figure 4D and Table S3). Dilution of the macrophage lysates prior to exposure to antibiotics did not affect the proportion of tolerant organisms (Figure S4B), excluding the possibility that tolerance was simply due to increased bacterial density at 96 hr (Figure 4B). Finally, we found that Mtb also develops macrophage-induced drug tolerance: 96 hr versus 2 hr infection yielded > 2.3-fold increase in INH survival and > 2.8-fold increase in RIF survival (Figure 4E and Table S3). Thus, macrophage residence rapidly induces Mm and Mtb to become tolerant to multiple drug classes.

Drug Tolerance Is Associated with a Replicating Intracellular Population

Current models invoke host-induced bacteriostasis as a mechanism for drug tolerance during infection. Indeed, both Mtb and Mm exhibit drug tolerance under conditions of slowed growth

(C) Enumeration of expanding and contracting granulomas over time. Differential region-specific outcomes of granulomas were statistically significant for changes occurring between days 7 and 11 ($p = 0.0022$), but not for changes occurring between days 4 and 7 ($p = 0.2360$, Fisher's exact test).

(D and E) Hematoxylin and eosin staining showing Mm in caseating granulomas in a 33-day-old fish that was infected at 1 dpf. Red and black arrows indicate granulomas in pronephros and liver, respectively. gl, gill; sb, swim bladder; sm, somite. Scale bar, 300 μm. Higher magnification of granulomas in boxed inset of (D) is shown on bottom-right of (E). Scale bar, 50 μm.

(F–I) Larvae infected with varying Mm inocula for 4 days were then treated with 290 μM INH or left untreated for an additional 3 days. Larvae were imaged at 4 and 7 dpi (0 and 3 dpt).

(F) Pre- and posttreatment $\log_{10}$ FPC values for individual larvae are plotted with data points from the same individual connected.

(G) Raw FPC values before and after treatment, percent change, and the presence of expanding and new foci are reported for representative fish indicated in (F).

(H and I) Fluorescence images of fish 11 (H) and fish 5 (I), as reported in (F) and (G), shown before and after treatment. Arrows, enlarging granulomas; arrowheads, new foci. Scale bars, 500 μm.

(J) A single larva was infected with 500 Mm constitutively expressing the Kaede photoactivatable GFP for 4 days. Composite red and green fluorescence images immediately after photoactivation of a granuloma (left) and 24 hr later (right). Arrows, photoactivated granuloma; arrowheads, single macrophages containing red fluorescent bacteria. Scale bar, 250 μm.

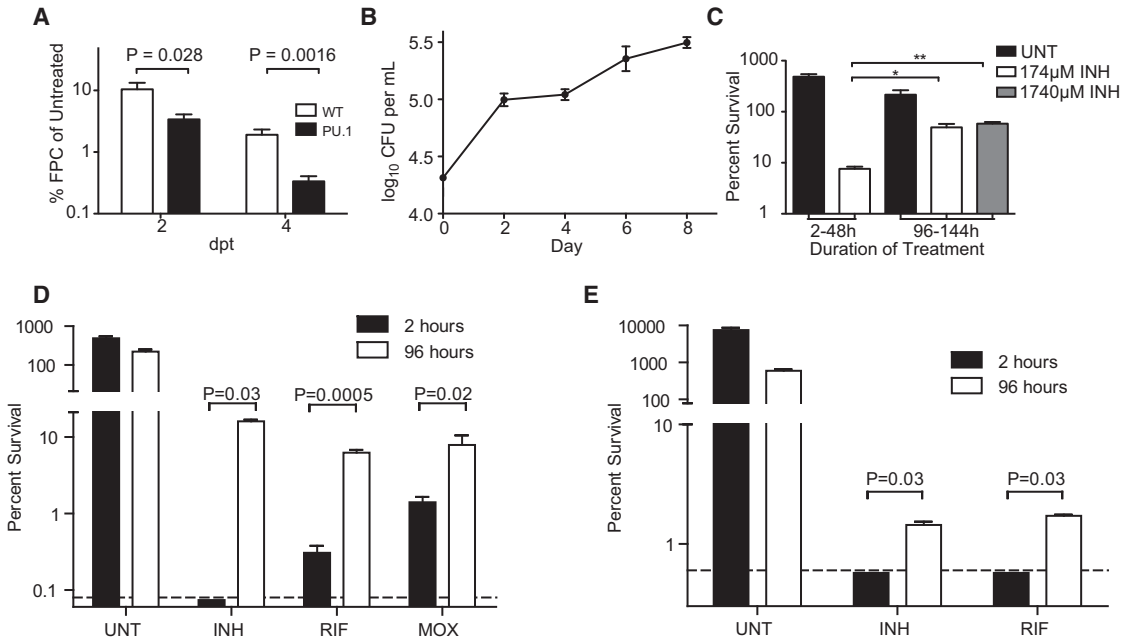

Figure 4. Antibiotic Tolerance Is Induced by Macrophage Residence

(A) Wild-type and PU.1-morphant larvae were infected with 300 Mm. One dpi larvae were treated with 290 μM INH or left untreated. Larvae were imaged at 2 and 4 dpt, and bacterial burdens were determined by FPC. For each time point, FPC of each treated larva was normalized to the mean FPC of the untreated control group. n = 20 wild-type or 12 PU.1 morphant larvae per group. p values determined using Student's t test.

(B and C) J774A.1 macrophages were infected with Mm and were left untreated or were treated with INH prior to lysis and enumeration of CFU.

(B) Growth of Mm in the untreated control wells.

(C) Survival of intracellular Mm upon exposure to 174 or 1740 μM INH during the time periods indicated (2–48 hr or 96–144 hr) prior to macrophage lysis and enumeration of CFU. Percent survival was compared using one-way ANOVA with Dunnett's posttest.

(D) Mm were used to infect THP-1 macrophages for 2 or 96 hr prior to being released by macrophage lysis. CFU were enumerated at the time of release and again following 48 hr exposure to 174 μM INH, 1.21 μM RIF, 7.48 μM MOX, or left untreated. For the purpose of display, values below the limit of detection (0.08%, dashed line) were arbitrarily set to 0.074%. p values were determined using Student's t test (RIF and MOX) or the Mann-Whitney rank test (INH).

(E) Mtb strain H37Rv was used to infect J774A.1 macrophages that were grown and treated as described for (D) except that the concentration of INH was 4.4 μM, reflecting the greater inherent susceptibility of this organism to INH. For the purpose of display, values below the limit of detection (0.6%, dashed line) were arbitrarily set to 0.57%. p values were determined using the Mann-Whitney rank test.

In all panels, error bars represent SEM.

in vitro (Figure S4C) (Paramasivan et al., 2005). Moreover, the net growth of Mm in macrophages appeared to decline slightly between 48 and 96 hr (Figure 4B), raising the possibility that tolerance might result from macrophage-induced bacteriostasis. However, both our zebrafish studies and prior human clinical data showed that bacteria expand and disseminate in vivo in the face of drug treatment. Thus, even if tolerance is initially associated with nongrowing persisters, they must somehow then retain the tolerance phenotype upon resuming growth.

To probe the replicative state of the tolerant bacteria, we manipulated intracellular growth by treating infected macrophages with dexamethasone (DEX), a broad-spectrum anti-inflammatory agent that increases net intracellular bacteria (Rook et al., 1987). DEX treatment resulted in a 2.1-fold increase in intracellular Mm at 96 hr that was accompanied by a 1.4-fold and 2.1-fold increase in the proportion of bacteria tolerant to INH and RIF, respectively (Figures 5A and 5B and Table S4). These experiments revealed that tolerance is not diminished by increased bacterial growth and suggested, rather, that it is enhanced in growing intracellular bacteria.

We then directly compared the numbers of drug-tolerant bacteria in nongrowing and growing intracellular populations. We transformed Mm with the unstable plasmid pBP10 that is lost at a constant rate from dividing, but not nondividing, mycobacteria (Figure S5) (Gill et al., 2009). Using Mm/pBP10, we showed the rate of plasmid loss per generation to be unchanged under different growth conditions (Figure S5 and Supplemental Experimental Procedures). We next used Mm/pBP10 to examine bacterial growth in macrophages. The generation time of the intracellular population was not decreased over the 96 hr assay period (Figure 5C and Figure S5). Furthermore, the apparent slowing of growth between 48 and 96 hr (Figure 4B) was, in fact, due to a large increase in bacterial death, which overshadowed a more modest increase in growth rate in this time period (Figure S5E).

We then compared the proportion of drug-tolerant bacteria in the population that had retained the plasmid (Kan^R; i.e., bacteria that had not yet replicated and daughter cells that had retained the plasmid upon replication) to that in the population that had lost the plasmid (Kan^S; i.e., completed at least one round of

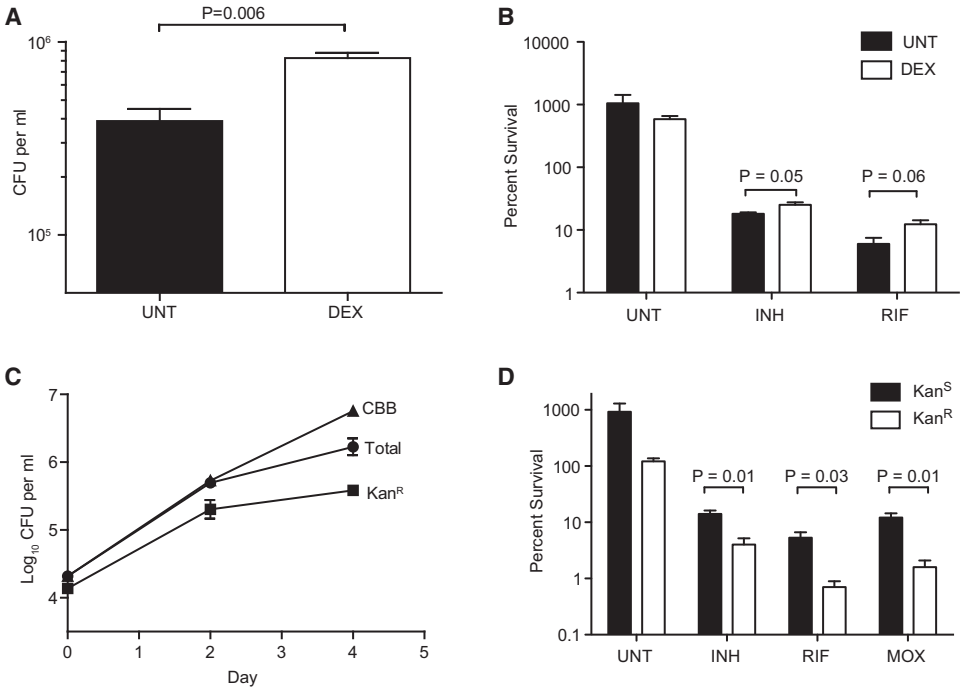

Figure 5. Growing Bacteria Are Enriched for Antibiotic Tolerance

(A and B) J774A.1 macrophages were infected with Mm and were treated with 100 nM dexamethasone at t = 0. Macrophages were lysed at 96 hpi to release bacteria.

(A) Total CFU at time of release.

(B) Percent survival of released bacteria upon 48 hr exposure to 174 μM INH, 1.21 μM RIF, or left untreated.

(C) J774A.1 macrophages were infected with Mm/pBP10 and total and Kan^R CFU enumerated at 48 and 96 hpi. The cumulative bacterial burden (CBB) was calculated as described in the Extended Experimental Procedures.

(D) Mm/pBP10 grown intracellularly for 96 hr (described in C) were released by macrophage lysis and then treated for an additional 48 hr with 174 μM INH, 1.21 μM RIF, 7.48 μM MOX, or left untreated prior to enumeration of total and Kan^R CFU. Kan^S CFU were calculated as the total CFU minus the mean Kan^R CFU.

In all panels, error bars represent SEM. p values were determined using Student's t test.

replication). Drug-tolerant bacteria were enriched in the Kan^S population: 3.5-fold for INH, 7.6-fold for RIF, and 7.6-fold for MOX (Figure 5D and Table S4). Together, these results suggested that drug tolerance was not associated with macrophage-induced bacteriostasis but, rather, that it was enhanced in the growing intracellular population.

Macrophage-Induced Bacterial Efflux Pumps Mediate Drug Tolerance

One explanation for the multiclass drug tolerance that we observed is a reduction in steady-state intrabacterial drug concentration, which could be achieved by decreased drug entry and/or increased efflux. The induction of efflux pumps causes single or multidrug resistance in many bacteria, including Mtb (De Rossi et al., 2006; Li and Nikaido, 2009; Louw et al., 2009), so we investigated their potential role in macrophage-induced tolerance. Mtb and Mm encode numerous efflux pumps that can mediate resistance to antitubercular drugs when overexpressed (Li and Nikaido, 2009). Efflux pump activity has been invoked to explain multiple aspects of drug resistance in mycobacteria: (1) intrinsic resistance, (2) acquired multidrug resistance, and (3) tolerance induced by antimicrobial exposure (De Rossi et al., 2006; Gupta et al., 2010; Louw et al., 2009; Morris et al., 2005; Viveiros et al., 2002). Moreover, several mycobacterial efflux pumps and their regulators are induced during macrophage infection (Fontán et al., 2008; Morris et al., 2005; Nguyen and Thompson, 2006; Ramón-García et al., 2009; Rohde et al., 2007; Schnappinger et al., 2003; Zähner et al., 2010). Finally, efflux pump inhibitors enhance the activity of certain drugs on drug-resistant Mtb; these include the currently approved pump inhibitors verapamil (VER), reserpine (RES), and thioridazine (Li and Nikaido, 2009).

To determine whether bacterial efflux pumps mediated macrophage-induced drug tolerance, we added subinhibitory VER and RES in conjunction with antibiotics to macrophage-released Mm and found that tolerance was reduced (Figures 6A and 6B and Table S5). VER produced a 15.6-fold reduction in INH survival and a 9.2-fold reduction in RIF survival; RES produced a 4.8-fold reduction in INH survival and a 7.9-fold reduction in RIF survival. These effects were specific to macrophage-induced tolerance: VER did not reduce stationary phase-induced tolerance to INH or RIF (Figure S6A).

In Mtb, VER reduced tolerance to RIF, but not to INH (Figure 6C and Table S5). RIF survival was reduced by 1.4-fold and 1.9-fold,

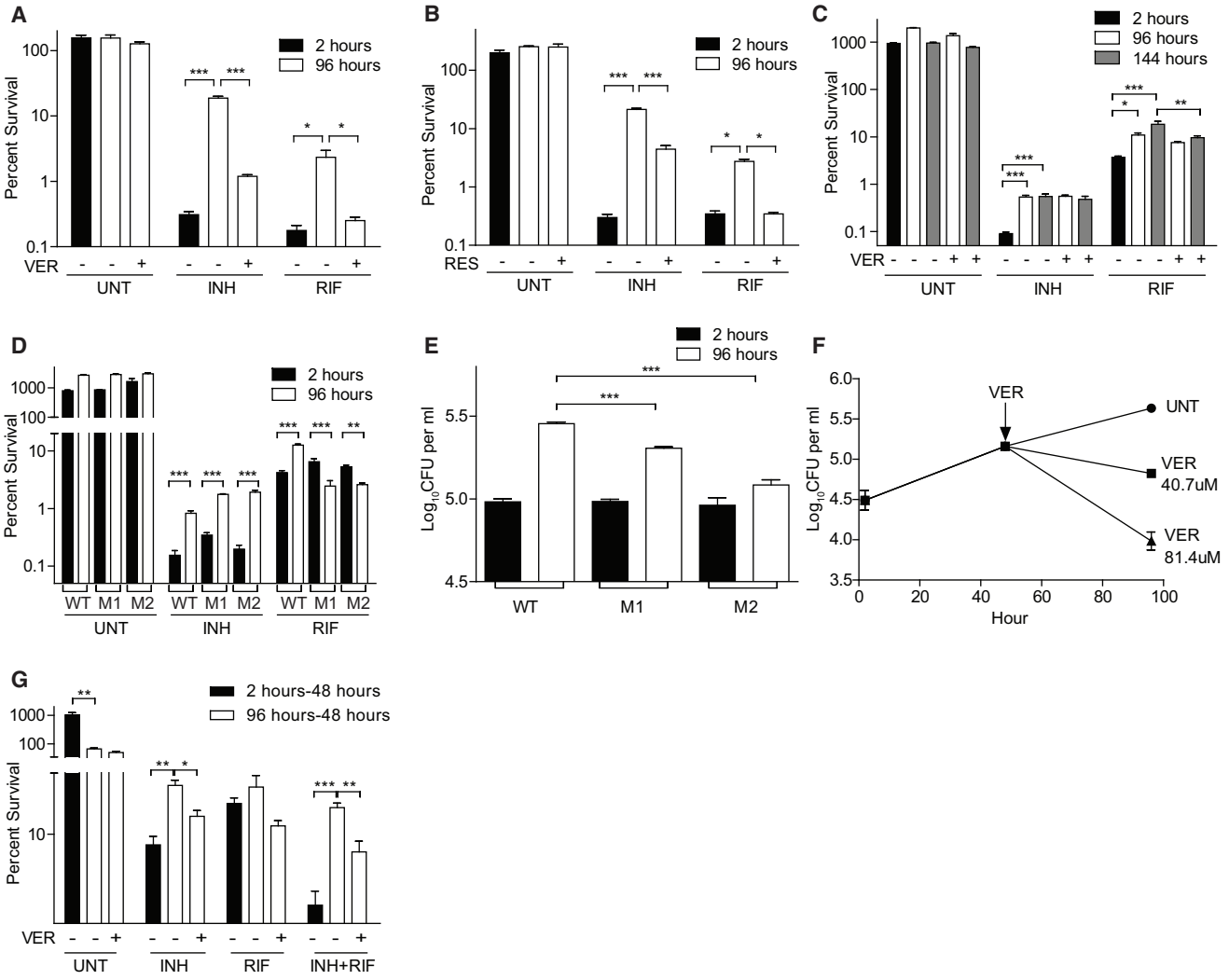

Figure 6. Bacterial Efflux Pumps Confer Tolerance within Macrophages

(A and B) THP-1 macrophages were infected with Mm and lysed at 2 or 96 hpi. The released bacteria were treated for an additional 48 hr with 174 μM INH, 1.21 μM RIF, or left untreated in the presence or absence of 81.4 μM verapamil (A) or 65.7 μM reserpine (B) prior to enumeration of CFU.

(C) THP-1 macrophages were infected with Mtb strain CDC1551 and lysed at 2, 96, or 144 hpi. The released bacteria were then treated with antibiotics for 48 hr as described in (A) except that the concentration of INH was 4.4 μM, as described for Figure 4E.

(D and E) THP-1 macrophages were infected with Mtb strains JHU1258c-715 ("M1"), JHU1258c-833 ("M2"), and the isogenic wild-type control, CDC 1551, for 2 or 96 hr prior to lysis and enumeration of CFU. (D) Released bacteria were treated as described in (C).

(F) THP-1 cells were infected with Mm for 48 hr prior to addition of 0 (UNT), 40.7, or 81.4 μM VER for an additional 48 hr. $p < 0.001$ using one-way ANOVA with Dunnett's posttest comparing each treatment group to the untreated control after 48 hr of VER treatment.

(G) THP-1 cells infected with Mm for 2 or 96 hr were incubated for an additional 48 hr with 174 μM INH, 1.21 μM RIF, or both and in the presence or absence of 40.7 μM VER. Cells were lysed and CFU were enumerated at the end of the 48 hr treatment. Percent survival was calculated relative to the mean intracellular counts present at the start of antibiotic exposure.

For all panels, error bars represent SEM. Significance testing was performed using one-way ANOVA with Dunnett's (A, B, D, and E) or Bonferroni (C and D) posttests.

respectively, in bacteria grown intracellularly for 96 and 144 hr prior to challenge. This result suggests that Mtb possesses VER-resistant pumps that are distinct from those used by Mm. Consistent with this idea, INH exposure induces transcription of more efflux pumps than does RIF in MDR-TB (Gupta et al., 2010). Moreover, drug-induced INH tolerance in Mtb is sensitive to RES, but not to VER (Colangeli et al., 2005; Viveiros et al., 2002).

Our data suggested that distinct efflux pumps mediate INH and RIF tolerance in Mtb. The Mtb Rv1258c efflux pump is transcriptionally induced upon: (1) macrophage infection (Morris et al., 2005; Schnappinger et al., 2003) and (2) exposure to subinhibitory concentrations of RIF, but not INH, in an Mtb isolate that is resistant to both drugs (Siddiqi et al., 2004). Hypothesizing that Rv1258c mediates macrophage-induced RIF tolerance, we

tested two Mtb strains with distinct transposon insertions in *Rv1258c*. After 96 hr of macrophage residence, both mutants retained INH, but lost RIF, tolerance (Figure 6D and Table S5). Indeed, they became hypersusceptible to RIF: whereas the wild-type had a 3.0-fold increase in tolerance, the mutants had 2.5- and 2.0-fold reductions in tolerance. Moreover, the mutants were compromised for intramacrophage growth (Figure 6E), suggesting that this efflux pump is required for both intracellular growth and RIF tolerance.

To confirm that the loss of tolerance in the *Rv1258c* mutants was not simply a function of intracellular growth attenuation, we tested two additional mutants with macrophage growth defects: Mm mutants lacking the RD1/ESX-1 secretion system or the cell surface/secreted Erp protein retained macrophage-inducible antibiotic tolerance (Figures S6B and S6C). The Erp mutant developed RIF tolerance despite being RIF hypersusceptible at baseline (Cosma et al., 2006b). This would suggest that efflux pump induction due to intracellular residence allowed the bacteria to extrude sufficient RIF to become more resistant than at baseline, despite growth attenuation. In contrast, the Rv1258c-deficient bacteria become hypersusceptible to RIF because their intracellular damage is coupled to an inability to expel RIF.

Finally, we showed that the Mtb *Rv1258c* mutants retained stationary phase-induced RIF tolerance, again showing specificity of this efflux pump in mediating macrophage-induced tolerance (Figure S6D). In sum, these results suggest that bacterial efflux pumps that are induced upon macrophage infection to promote intracellular bacterial growth also serve to mediate drug tolerance. This mechanistic understanding explains the enrichment of tolerant bacteria in the growing intracellular population.

VER Reduces Intracellular Mm Growth and Tolerance

If VER reduces tolerance by inhibiting bacterial efflux pumps induced upon intracellular residence, it should reduce tolerance when administered directly to infected macrophages. It should also inhibit intracellular growth, as suggested by the *Rv1258c* mutants. Indeed, efflux pump and potassium transport inhibitors have been found to promote intracellular killing of multidrug-resistant Mtb (Amaral et al., 2007). We similarly found that incubation of Mm-infected macrophages with VER reduced intracellular bacterial growth at concentrations that did not impact bacteria in axenic culture (Figure 6F and Figure S6A). Incubation of infected macrophages with VER also inhibited tolerance (Figure 6G). The 96 hr Mm-infected macrophages were treated with INH alone or INH and VER for an additional 48 hr before lysis and bacterial enumeration; the addition of VER reduced tolerance by 2.0-fold (Figure 6G and Table S5). Finally, when added to a synergistic combination of INH and RIF, VER further reduced tolerance by 2.2-fold (Figure 6G and Table S5), suggesting the potential of VER to increase the efficacy of existing treatment regimens. Taken together, the finding that mutations in *Rv1258c* and treatment with the efflux pump inhibitor VER lead to the same two phenotypes (growth attenuation and loss of tolerance) indicates that efflux pumps are required for both processes. Moreover, the observation that VER treatment phenocopies the *Rv1258c* mutation argues that it is the loss of Rv1258c function in the mutants, rather than polar effects on downstream genes, that is responsible for the observed phenotypes.

Macrophage-Induced Tolerance Persists after Bacteria Are Rendered Extracellular

Both the zebrafish larval model and the human EBA studies reveal the existence of tolerant bacteria. However, in contrast to the intracellular bacteria present in the larvae, the tolerant bacteria assessed in the human studies are thought to be predominantly extracellular, residing within the necrotic cores of open cavitary lesions (Figure S1). Necrosis results from death of the granuloma's macrophage core and is sustained by continued influx and lysis of infected and uninfected macrophages (Cosma et al., 2004; Dannenberg, 2003). Thus, for macrophage-induced tolerance to play a significant role in human cavitary TB, it must persist after the bacteria are rendered extracellular by macrophage lysis. To test this model, we lysed Mm out of macrophages and monitored the proportion of tolerant organisms over time. Mm retained tolerance for at least 120 hr after macrophage release despite continued replication in the lysate (Figure S7A and S7B). Whether tolerance is retained due to slow turnover of the efflux pump or persistence of the original macrophage stimulus in the lysates remains to be determined. Regardless of the mechanism, these findings argue that extracellular bacteria in cavitary TB may be rendered tolerant by prior growth in macrophages.

DISCUSSION

Drug tolerance presents a significant challenge to the eradication of TB. Here, we exploit complementary infection models to demonstrate that macrophages and granulomas both play a role in the induction and expansion of drug-tolerant bacteria.

The zebrafish larval model has enabled reassessment of fundamental dogmas about the role of macrophages and granulomas in TB pathogenesis (Davis and Ramakrishnan, 2009; Tobin and Ramakrishnan, 2008; Tobin et al., 2010; Volkman et al., 2010). These studies found that, rather than serving as strictly host-protective structures, granulomas are co-opted by mycobacteria for their expansion and dissemination. We now show that tolerant bacteria arising within individual macrophages similarly exploit granulomas for their amplification and dissemination during the course of drug treatment. This finding helps to explain decades-old observations that human TB lesions can expand, and new ones appear, in the face of overall clinical and radiological response (Akira et al., 2000; Bobrowitz, 1980; Canetti, 1955).

The core finding of this study is that drug-tolerant bacteria originate in macrophages dependent on the activity of bacterial efflux pumps (Figure 7). Within a few days of macrophage infection, a bacterial subpopulation arises that manifests tolerance to multiple drugs independent of drug exposure. The association between intramacrophage growth and drug tolerance suggests that a common mechanism promotes both. This is borne out by our finding that Rv1258c is required for both macrophage growth and intracellular RIF tolerance in Mtb. The activation of bacterial efflux pumps in response to membrane and oxidative stress and antimicrobial peptides in vitro (Morris et al., 2005;

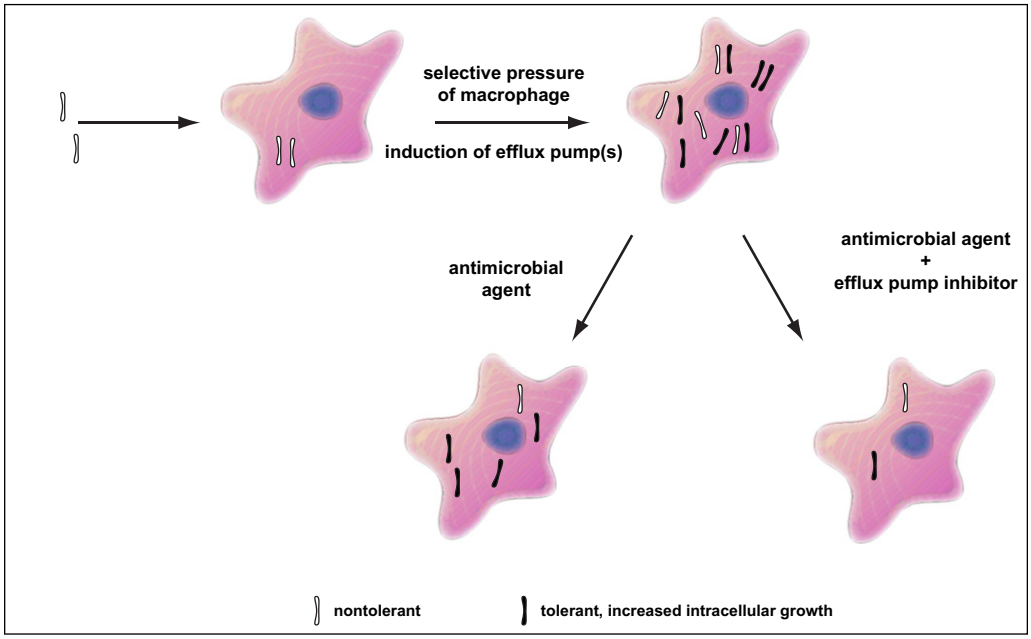

Figure 7. Model for the Mechanism of Antibiotic Tolerance in TB and Its Treatment

Nontolerant bacteria are phagocytosed by macrophages soon after infection wherein they induce efflux pumps to counter macrophage defenses. These efflux pumps render bacteria tolerant to multiple antitubercular drugs. The tolerant bacteria are associated with the growing population because of their enhanced ability to counter macrophage defenses. Antitubercular drug treatment spares tolerant bacteria, and the addition of efflux pump inhibitors reduces their numbers.

Nguyen and Thompson, 2006; Ramón-García et al., 2009; Zähner et al., 2010) suggests that their induction during intracellular residence may protect the bacteria from these same conditions in vivo. For example, efflux pumps mediate intrinsic resistance of *Neisseria meningitidis* to human antimicrobial peptides (Tzeng et al., 2005). The finding that DEX-treated macrophages induce tolerance may shed some light on the intracellular stimuli involved. DEX treatment suppresses macrophage oxidative bursts while preserving antimicrobial peptide expression (Duits et al., 2001; Ehrchen et al., 2007). Antimicrobial peptides, which are induced in Mtb-infected human macrophages and are required for macrophage antimycobacterial activity (Liu et al., 2007; Rivas-Santiago et al., 2008), may mediate the induction of bacterial efflux pumps and thereby tolerance.

Our in vivo results show that tolerant bacteria arise within a subset of infected macrophages during treatment. This may be due to macrophage heterogeneity, again underscoring the complexity of the macrophage-*Mycobacterium* interface. Individual macrophages may cause distinct and/or differential induction of bacterial efflux pumps and, thus, variable tolerance within the bacterial population. Additionally, antibiotics have long been thought to act in co-operation with cellular host defenses, an idea further supported by the increasing recognition of the complex, multidimensional mechanisms of antibiotic activity (Kohanski et al., 2010).

How do our findings relate to human clinical studies? Among the readily cultivable bacilli in the sputum of humans with active cavitary TB, two distinct populations have been described: drug susceptible and drug tolerant (Jindani et al., 2003). The metabolic status of the tolerant population has been the source of much debate. Spurred by our discovery of early tolerance in zebrafish larvae, we revisited human EBA and radiological studies and realized that growing, tolerant populations must mediate the progression and expansion of tubercular lesions that occur in the face of treatment (Bobrowitz, 1980; Jindani et al., 2003). The association between tolerance and intracellular growth in the zebrafish larval and macrophage models provides a mechanism for the earlier human studies. Further strengthening this link is our finding that tolerance persists for days after the bacteria are released from macrophages, suggesting that the bacteria present in the necrotic core of macrophage-lined cavities may utilize similar tolerance mechanisms.

Slowly growing bacteria that are not cultivable under standard conditions have also been observed in human sputum (Garton et al., 2008; Mukamolova et al., 2010). These too appear to be drug tolerant, but their relative impact on treatment duration and clinical relapse is unclear (Mukamolova et al., 2010). Importantly, tolerance models centered on nonreplicating bacteria do not account for the recent finding that diarylquinolones, which are equally bactericidal for exponentially growing and dormant bacteria in culture (Koul et al., 2008), only shorten the time to cure from 6 months to 4 in the mouse model of TB, which features slowed bacterial growth (Ibrahim et al., 2009; Muñoz-Elías et al., 2005). Although this shortening may be extremely important clinically, it does not support the notion that tolerance, and thus the long duration required for therapy, is mediated solely by dormant bacterial populations. One possibility is that the growing, tolerant bacteria revealed in this work are responsible for the substantial residual tolerance observed after diarylquinolone-containing therapies.

In summary, we have identified a population of drug-tolerant bacteria that are likely to be substantially present in TB patients as they are induced by macrophages, which host dynamic mycobacterial populations throughout infection. Current drug discovery efforts, with their emphasis on quiescent tolerant bacteria, fail to take into account the role of this population in tolerance. Our identification of pharmacological measures to reduce the numbers of growing tolerant bacteria suggests an approach to further shorten TB chemotherapy. Our finding that the same pump mediates both growth and tolerance suggests that the identification of more potent specific inhibitors with a dual bacterial killing mechanism is possible. Indeed, some are already being tested against Rv1258c (Sharma et al., 2010). Ultimately, the best assessment of whether targeting these newly discovered tolerant bacteria is the key to truly short-course chemotherapy will come from clinical trials using efflux pump inhibitors like VER.

Finally, the tolerance mechanisms and counter strategies that we describe for mycobacteria may be relevant to other intracellular pathogens. Indeed, macrophage-induced tolerance to multiple drug classes is described for *Legionella pneumophila*, an agent of pneumonia (Barker et al., 1995). Thus, our findings may have relevance for *Legionella* as well as other recalcitrant intracellular pathogens that produce serious and often relapsing infections in which tolerance is a barrier to therapy.

EXPERIMENTAL PROCEDURES

Bacterial Strains and Methods

M. marinum strain M (ATCC BAA-535) and its fluorescent derivatives have been described (Cosma et al., 2006a; Davis and Ramakrishnan, 2009). A spontaneous INH-resistant mutant identified in our laboratory (KA1) was found to have increased resistance to INH (MIC 64 μg/ml), and the *katG* locus was subsequently sequenced. Plasmid pBP10 (gift of D. Sherman, Seattle Biomed) was transformed into strain M to yield strain KA2, referred to in the text as Mm/pBP10. Mm were grown in standard media (see Extended Experimental Procedures) and prepared for experimental manipulations by growth to midlog phase, followed by passage through a sterile 5 μM filter to yield a single cell suspension. INH susceptibility of bacteria isolated from INH-treated larvae was verified by patching all outgrown colonies onto 7H10 agar containing 10, 20, and 40 μg/ml INH and comparing growth to that of the parental strain. The INH MIC of three colonies was confirmed to be identical to strain M.

Mtb strain H37Rv was from D. Sherman (Seattle Biomed). Mtb strains JHU1258c-715 and JHU1258c-833 (harboring transposon insertions at positions 715 and 833, respectively, in the *Rv1258c* ORF) and the wild-type parent strain CDC1551 were from W.R. Bishai and G. Lamichhane (Johns Hopkins University) (Lamichhane et al., 2003). Mtb were grown to midlog phase in standard medium prior to infection.

Zebrafish Infections

Wild-type AB zebrafish were from our laboratory stock, and PU.1 morphant embryos have been described (Clay et al., 2007). Larvae were infected via caudal vein injections at 36–48 hr postfertilization (Cosma et al., 2006a) and maintained as described for individual experiments with feeding instituted at day 14 dpf (Davis and Ramakrishnan, 2009).

Microscopy

Wide-field fluorescence microscopy was performed using a Nikon E600 equipped with a Nikon D-FL-E fluorescence unit with a 100 W Mercury lamp. Wide-field fluorescence images were captured using a CoolSnap HQ CCD camera (Photometrics) with MetaMorph 7.1 (Molecular Devices).

Fluorescent Pixel Count

Quantification of infection with fluorescent Mm using images of individual embryos was performed using custom-made MATLAB software developed in house. In brief, in each image, the number of pixels with a fluorescence intensity greater than the brightest pixel observed in images of control uninfected embryos is counted. This count represents the total fluorescent area (in pixels) for each infected larva.

Calculation of Early Bactericidal Activity

FPC counts were $\log_{10}$ transformed, and for each larva, the difference between each day's measurement and the initial burden was calculated. EBAs over defined intervals were calculated by taking the mean and SD of the $\Delta \log_{10}$ FPC values calculated for individual larvae.

Macrophage Growth and Infection

J774A.1 and THP-1 macrophages were grown in DMEM and RPMI, respectively, supplemented with 10% FBS and 1% L-glutamine. THP-1 cells were differentiated with phorbol 12-myristate 13-acetate for 48 hr prior to infection. 1×10^5 J774A.1 or 5×10^5 THP-1 macrophages were infected at an MOI of 1.5 for 2–3 hr at 33°C (for Mm) or an MOI of 1 for 2–3 hr at 37°C (for Mtb). Cells were washed with medium and then 20 (for Mm) or 6 (for Mtb) μg/ml STM was added (t = 0) for the duration of the intracellular growth. Medium was changed daily. Macrophages were lysed with 0.1% Triton X-100 for intracellular growth quantization. To lyse macrophages and release bacteria for subsequent tolerance assessment, each well was first washed once with 1 × PBS and once with diH_2O, with the latter wash being removed immediately. Then, 200 μl of diH_20 was added and the cells incubated for 15 min to lyse macrophages. Finally, 800 μl of 1.25× concentrated 7H9 medium (see Extended Experimental Procedures) was added and the wells scraped gently with a pipette tip to release all macrophages. CFU were enumerated from triplicate wells on supplemented 7H10 agar. For determination of antibiotic killing, the percent survival was calculated by dividing the CFU for each well by the mean CFU present prior to treatment.

Statistics

Statistical analyses were performed using Prism 5.01 (GraphPad). For data sets requiring $\log_{10}$ transformation prior to ANOVA, embryos with no detectable fluorescence above background, or with no detectable CFU were assigned a value of 0.9, with 1 being the limit of detection, prior to $\log_{10}$ transformation. A Mann Whitney rank test was used when values in one group were all below the limit of detection. Posttest p values are as follows: $^*p < 0.05$; $^{**}p < 0.01$; $^{***}p < 0.001$.

SUPPLEMENTAL INFORMATION

Supplemental Information includes Extended Experimental Procedures, seven figures, and five tables and can be found with this article online at doi:10.1016/j.cell.2011.02.022.

ACKNOWLEDGMENTS

We thank D.R. Sherman for the gift of pBP10, advice, and the use of the BSL-3 facilities at Seattle BioMed; the members of his laboratory, especially R. Liao and J. Pang, for help in using the BSL-3 facilities; M. Nixon for advice in analyzing the unstable plasmid data; W.R. Bishai and G. Lamichhane for providing the Mtb *Rv1258c* mutants through the Tuberculosis Animal Research and Gene Evaluation Taskforce (NIH/NIAID N01 AI30036); E. Nuermberger and P. Donald for sharing knowledge and insights about TB drugs; B. Cormack and M. Troll for discussion; J.M. Davis and C.T. Yang for technical advice; J. Ray and H. Volkman for figure design and preparation; and S. Phillips and T. Pecor for technical assistance. This work was supported by a Gates Foundation TB drug accelerator grant; a University of Washington Royalty Research Fund Grant; a Burroughs Wellcome Foundation Pathogenesis of Infectious Diseases award; NIH grants RO1 AI036396, RO1 AI54503, and U54AI057141 to L.R.; NIH grant T32 AI55396 to K.N.A.; a Levinson Emerging Scholars Program Grant, a Mary Gates Endowment Grant, and a Washington

NASA Space Grant to K.W.; a Pfizer Fellowship in Infectious Diseases and NIH grant K08 AI076620 to L.E.C.; and NIH grants 5R21 AI073328-02 and 5R21 AI078189-02 to P.H.E. L.R. is a recipient of the NIH Director's Pioneer Award and a consultant for Sanofi Aventis.

Received: July 20, 2010
Revised: November 9, 2010
Accepted: February 1, 2011
Published online: March 3, 2011

REFERENCES

Akira, M., Sakatani, M., and Ishikawa, H. (2000). Transient radiographic progression during initial treatment of pulmonary tuberculosis: CT findings. J. Comput. Assist. Tomogr. *24*, 426–431.

Amaral, L., Martins, M., and Viveiros, M. (2007). Enhanced killing of intracellular multidrug-resistant Mycobacterium tuberculosis by compounds that affect the activity of efflux pumps. J. Antimicrob. Chemother. *59*, 1237–1246.

Aubry, A., Chosidow, O., Caumes, E., Robert, J., and Cambau, E. (2002). Sixty-three cases of Mycobacterium marinum infection: clinical features, treatment, and antibiotic susceptibility of causative isolates. Arch. Intern. Med. *162*, 1746–1752.

Barker, J., Scaife, H., and Brown, M.R. (1995). Intraphagocytic growth induces an antibiotic-resistant phenotype of Legionella pneumophila. Antimicrob. Agents Chemother. *39*, 2684–2688.

Barry, C.E., III, Boshoff, H.I., Dartois, V., Dick, T., Ehrt, S., Flynn, J., Schnappinger, D., Wilkinson, R.J., and Young, D. (2009). The spectrum of latent tuberculosis: rethinking the biology and intervention strategies. Nat. Rev. Microbiol. *7*, 845–855.

Belanger, A.E., Besra, G.S., Ford, M.E., Mikusová, K., Belisle, J.T., Brennan, P.J., and Inamine, J.M. (1996). The embAB genes of Mycobacterium avium encode an arabinosyl transferase involved in cell wall arabinan biosynthesis that is the target for the antimycobacterial drug ethambutol. Proc. Natl. Acad. Sci. USA *93*, 11919–11924.

Bobrowitz, I.D. (1980). Reversible roentgenographic progression in the initial treatment of pulmonary tuberculosis. Am. Rev. Respir. Dis. *121*, 735–742.

Canetti, G. (1955). The Tubercle Bacillus in the Pulmonary Lesion of Man; Histobacteriology and Its Bearing on the Therapy of Pulmonary Tuberculosis (New York: Springer).

Clay, H., Davis, J.M., Beery, D., Huttenlocher, A., Lyons, S.E., and Ramakrishnan, L. (2007). Dichotomous role of the macrophage in early Mycobacterium marinum infection of the zebrafish. Cell Host Microbe *2*, 29–39.

Colangeli, R., Helb, D., Sridharan, S., Sun, J., Varma-Basil, M., Hazbón, M.H., Harbacheuski, R., Megjugorac, N.J., Jacobs, W.R., Jr., Holzenburg, A., et al. (2005). The Mycobacterium tuberculosis iniA gene is essential for activity of an efflux pump that confers drug tolerance to both isoniazid and ethambutol. Mol. Microbiol. *55*, 1829–1840.

Connolly, L.E., Edelstein, P.H., and Ramakrishnan, L. (2007). Why is long-term therapy required to cure tuberculosis? PLoS Med. *4*, e120.

Cosma, C.L., Humbert, O., and Ramakrishnan, L. (2004). Superinfecting mycobacteria home to established tuberculous granulomas. Nat. Immunol. *5*, 828–835.

Cosma, C.L., Davis, J.M., Swaim, L.E., Volkman, H., and Ramakrishnan, L. (2006a). Zebrafish and Frog Models of Mycobacterium marinum Infection. In Current Protocols in Microbiology, R. Coico, T. Kowalik, J. Quarles, B. Stevenson, and R. Taylor, eds. (New York: John Wiley and Sons).

Cosma, C.L., Klein, K., Kim, R., Beery, D., and Ramakrishnan, L. (2006b). Mycobacterium marinum Erp is a virulence determinant required for cell wall integrity and intracellular survival. Infect. Immun. *74*, 3125–3133.

Dannenberg, A.M., Jr. (2003). Macrophage turnover, division and activation within developing, peak and "healed" tuberculous lesions produced in rabbits by BCG. Tuberculosis (Edinb.) *83*, 251–260.

Davis, J.M., and Ramakrishnan, L. (2009). The role of the granuloma in expansion and dissemination of early tuberculous infection. Cell *136*, 37–49.

De Rossi, E., Aínsa, J.A., and Riccardi, G. (2006). Role of mycobacterial efflux transporters in drug resistance: an unresolved question. FEMS Microbiol. Rev. *30*, 36–52.

Decostere, A., Hermans, K., and Haesebrouck, F. (2004). Piscine mycobacteriosis: a literature review covering the agent and the disease it causes in fish and humans. Vet. Microbiol. *99*, 159–166.

de Steenwinkel, J.E., de Knegt, G.J., Ten Kate, M.T., van Belkum, A., Verbrugh, H.A., Kremer, K., van Soolingen, D., and Bakker-Woudenberg, I.A. (2010). Time-kill kinetics of anti-tuberculosis drugs, and emergence of resistance, in relation to metabolic activity of Mycobacterium tuberculosis. J. Antimicrob. Chemother. *65*, 2582–2589.

Donald, P.R., and Diacon, A.H. (2008). The early bactericidal activity of anti-tuberculosis drugs: a literature review. Tuberculosis (Edinb.) *88* (*Suppl 1*), S75–S83.

Donald, P.R., and McIlleron, H. (2009). Antituberculosis drugs. In Tuberculosis: A Comprehensive Clinical Reference, H. Schaaf and A. Zumla, eds. (London, UK: Saunders Elsevier), pp. 608–617.

Duits, L.A., Rademaker, M., Ravensbergen, B., van Sterkenburg, M.A., van Strijen, E., Hiemstra, P.S., and Nibbering, P.H. (2001). Inhibition of hBD-3, but not hBD-1 and hBD-2, mRNA expression by corticosteroids. Biochem. Biophys. Res. Commun. *280*, 522–525.

Ehrchen, J., Steinmüller, L., Barczyk, K., Tenbrock, K., Nacken, W., Eisenacher, M., Nordhues, U., Sorg, C., Sunderkötter, C., and Roth, J. (2007). Glucocorticoids induce differentiation of a specifically activated, anti-inflammatory subtype of human monocytes. Blood *109*, 1265–1274.

Fontán, P.A., Aris, V., Alvarez, M.E., Ghanny, S., Cheng, J., Soteropoulos, P., Trevani, A., Pine, R., and Smith, I. (2008). Mycobacterium tuberculosis sigma factor E regulon modulates the host inflammatory response. J. Infect. Dis. *198*, 877–885.

Garton, N.J., Waddell, S.J., Sherratt, A.L., Lee, S.M., Smith, R.J., Senner, C., Hinds, J., Rajakumar, K., Adegbola, R.A., Besra, G.S., et al. (2008). Cytological and transcript analyses reveal fat and lazy persister-like bacilli in tuberculous sputum. PLoS Med. *5*, e75.

Gill, W.P., Harik, N.S., Whiddon, M.R., Liao, R.P., Mittler, J.E., and Sherman, D.R. (2009). A replication clock for Mycobacterium tuberculosis. Nat. Med. *15*, 211–214.

Gupta, A.K., Katoch, V.M., Chauhan, D.S., Sharma, R., Singh, M., Venkatesan, K., and Sharma, V.D. (2010). Microarray analysis of efflux pump genes in multidrug-resistant Mycobacterium tuberculosis during stress induced by common anti-tuberculous drugs. Microb. Drug Resist. *16*, 21–28.

Ibrahim, M., Truffot-Pernot, C., Andries, K., Jarlier, V., and Veziris, N. (2009). Sterilizing activity of R207910 (TMC207)-containing regimens in the murine model of tuberculosis. Am. J. Respir. Crit. Care Med. *180*, 553–557.

Jindani, A., Doré, C.J., and Mitchison, D.A. (2003). Bactericidal and sterilizing activities of antituberculosis drugs during the first 14 days. Am. J. Respir. Crit. Care Med. *167*, 1348–1354.

Kohanski, M.A., Dwyer, D.J., and Collins, J.J. (2010). How antibiotics kill bacteria: from targets to networks. Nat. Rev. Microbiol. *8*, 423–435.

Koul, A., Vranckx, L., Dendouga, N., Balemans, W., Van den Wyngaert, I., Vergauwen, K., Göhlmann, H.W., Willebrords, R., Poncelet, A., Guillemont, J., et al. (2008). Diarylquinolines are bactericidal for dormant mycobacteria as a result of disturbed ATP homeostasis. J. Biol. Chem. *283*, 25273–25280.

Lamichhane, G., Zignol, M., Blades, N.J., Geiman, D.E., Dougherty, A., Grosset, J., Broman, K.W., and Bishai, W.R. (2003). A postgenomic method for predicting essential genes at subsaturation levels of mutagenesis: application to Mycobacterium tuberculosis. Proc. Natl. Acad. Sci. USA *100*, 7213–7218.

Li, X.Z., and Nikaido, H. (2009). Efflux-mediated drug resistance in bacteria: an update. Drugs *69*, 1555–1623.

Liu, P.T., Stenger, S., Tang, D.H., and Modlin, R.L. (2007). Cutting edge: vitamin D-mediated human antimicrobial activity against Mycobacterium tuberculosis is dependent on the induction of cathelicidin. J. Immunol. *179*, 2060–2063.

Louw, G.E., Warren, R.M., Gey van Pittius, N.C., McEvoy, C.R., Van Helden, P.D., and Victor, T.C. (2009). A balancing act: efflux/influx in mycobacterial drug resistance. Antimicrob. Agents Chemother. *53*, 3181–3189.

Morris, R.P., Nguyen, L., Gatfield, J., Visconti, K., Nguyen, K., Schnappinger, D., Ehrt, S., Liu, Y., Heifets, L., Pieters, J., et al. (2005). Ancestral antibiotic resistance in Mycobacterium tuberculosis. Proc. Natl. Acad. Sci. USA *102*, 12200–12205.

Mukamolova, G.V., Turapov, O., Malkin, J., Woltmann, G., and Barer, M.R. (2010). Resuscitation-promoting factors reveal an occult population of tubercle Bacilli in Sputum. Am. J. Respir. Crit. Care Med. *181*, 174–180.

Muñoz-Elías, E.J., Timm, J., Botha, T., Chan, W.T., Gomez, J.E., and McKinney, J.D. (2005). Replication dynamics of Mycobacterium tuberculosis in chronically infected mice. Infect. Immun. *73*, 546–551.

Nguyen, L., and Thompson, C.J. (2006). Foundations of antibiotic resistance in bacterial physiology: the mycobacterial paradigm. Trends Microbiol. *14*, 304–312.

Paramasivan, C.N., Sulochana, S., Kubendiran, G., Venkatesan, P., and Mitchison, D.A. (2005). Bactericidal action of gatifloxacin, rifampin, and isoniazid on logarithmic- and stationary-phase cultures of Mycobacterium tuberculosis. Antimicrob. Agents Chemother. *49*, 627–631.

Ramón-García, S., Martín, C., Thompson, C.J., and Aínsa, J.A. (2009). Role of the Mycobacterium tuberculosis P55 efflux pump in intrinsic drug resistance, oxidative stress responses, and growth. Antimicrob. Agents Chemother. *53*, 3675–3682.

Rich, A.R. (1946). The Pathogenesis of Tuberculosis, Second Edition (Springfield, IL: Charles C. Thomas).

Rivas-Santiago, B., Hernandez-Pando, R., Carranza, C., Juarez, E., Contreras, J.L., Aguilar-Leon, D., Torres, M., and Sada, E. (2008). Expression of cathelicidin LL-37 during Mycobacterium tuberculosis infection in human alveolar macrophages, monocytes, neutrophils, and epithelial cells. Infect. Immun. *76*, 935–941.

Rohde, K.H., Abramovitch, R.B., and Russell, D.G. (2007). Mycobacterium tuberculosis invasion of macrophages: linking bacterial gene expression to environmental cues. Cell Host Microbe *2*, 352–364.

Rook, G.A., Steele, J., Ainsworth, M., and Leveton, C. (1987). A direct effect of glucocorticoid hormones on the ability of human and murine macrophages to control the growth of M. tuberculosis. Eur. J. Respir. Dis. *71*, 286–291.

Sacchettini, J.C., Rubin, E.J., and Freundlich, J.S. (2008). Drugs versus bugs: in pursuit of the persistent predator Mycobacterium tuberculosis. Nat. Rev. Microbiol. *6*, 41–52.

Sandgren, A., Strong, M., Muthukrishnan, P., Weiner, B.K., Church, G.M., and Murray, M.B. (2009). Tuberculosis drug resistance mutation database. PLoS Med. *6*, e2.

Schnappinger, D., Ehrt, S., Voskuil, M.I., Liu, Y., Mangan, J.A., Monahan, I.M., Dolganov, G., Efron, B., Butcher, P.D., Nathan, C., and Schoolnik, G.K. (2003). Transcriptional Adaptation of Mycobacterium tuberculosis within Macrophages: Insights into the Phagosomal Environment. J. Exp. Med. *198*, 693–704.

Sharma, S., Kumar, M., Sharma, S., Nargotra, A., Koul, S., and Khan, I.A. (2010). Piperine as an inhibitor of Rv1258c, a putative multidrug efflux pump of Mycobacterium tuberculosis. J. Antimicrob. Chemother. *65*, 1694–1701.

Siddiqi, N., Das, R., Pathak, N., Banerjee, S., Ahmed, N., Katoch, V.M., and Hasnain, S.E. (2004). Mycobacterium tuberculosis isolate with a distinct genomic identity overexpresses a tap-like efflux pump. Infection *32*, 109–111.

Tobin, D.M., and Ramakrishnan, L. (2008). Comparative pathogenesis of Mycobacterium marinum and Mycobacterium tuberculosis. Cell. Microbiol. *10*, 1027–1039.

Tobin, D.M., Vary, J.C., Jr., Ray, J.P., Walsh, G.S., Dunstan, S.J., Bang, N.D., Hagge, D.A., Khadge, S., King, M.C., Hawn, T.R., et al. (2010). The lta4h locus modulates susceptibility to mycobacterial infection in zebrafish and humans. Cell *140*, 717–730.

Tzeng, Y.L., Ambrose, K.D., Zughaier, S., Zhou, X., Miller, Y.K., Shafer, W.M., and Stephens, D.S. (2005). Cationic antimicrobial peptide resistance in Neisseria meningitidis. J. Bacteriol. *187*, 5387–5396.

Viveiros, M., Portugal, I., Bettencourt, R., Victor, T.C., Jordaan, A.M., Leandro, C., Ordway, D., and Amaral, L. (2002). Isoniazid-induced transient high-level resistance in Mycobacterium tuberculosis. Antimicrob. Agents Chemother. *46*, 2804–2810.

Volkman, H.E., Clay, H., Beery, D., Chang, J.C., Sherman, D.R., and Ramakrishnan, L. (2004). Tuberculous granuloma formation is enhanced by a mycobacterium virulence determinant. PLoS Biol. *2*, e367.

Volkman, H.E., Pozos, T.C., Zheng, J., Davis, J.M., Rawls, J.F., and Ramakrishnan, L. (2010). Tuberculous granuloma induction via interaction of a bacterial secreted protein with host epithelium. Science *327*, 466–469.

Warner, D.F., and Mizrahi, V. (2006). Tuberculosis chemotherapy: the influence of bacillary stress and damage response pathways on drug efficacy. Clin. Microbiol. Rev. *19*, 558–570.

Zähner, D., Zhou, X., Chancey, S.T., Pohl, J., Shafer, W.M., and Stephens, D.S. (2010). Human antimicrobial peptide LL-37 induces MefE/Mel-mediated macrolide resistance in Streptococcus pneumoniae. Antimicrob. Agents Chemother. *54*, 3516–3519.